Myostatin deficiency partially rescues the bone phenotype of osteogenesis imperfecta model mice

A. K. Oestreich[1], **S. M. Carleton**[2], **X. Yao**[3], **B. A. Gentry**[4], **C. E. Raw**[2], **M. Brown**[5], **F. M. Pfeiffer**[6], **Y. Wang**[3], **C. L. Phillips**[2,7]

[1]Department of Biological Sciences, University of Missouri, Columbia, MO 65211, USA

[2]Department of Biochemistry, University of Missouri, Columbia, MO 65211, USA

[3]Department of Oral and Craniofacial Sciences, School of Dentistry, University of Missouri-Kansas City, Kansas City, MO 64108, USA

[4]Department of Veterinary Pathobiology, University of Missouri, Columbia, MO 65211, USA

[5]Department of Biomedical Sciences and Physical Therapy Program, University of Missouri, Columbia, MO 65211, USA

[6]Department of Orthopaedic Surgery and Bioengineering, University of Missouri, Columbia, MO 65211, USA

[7]Department of Child Health, University of Missouri, 117 Schweitzer Hall, Columbia, MO 65211, USA

Abstract

Summary—Mice with osteogenesis imperfecta (+/*oim*), a disorder of bone fragility, were bred to mice with muscle over growth to test whether increasing muscle mass genetically would improve bone quality and strength. The results demonstrate that femora from mice carrying both mutations have greater mechanical integrity than their +/*oim* littermates.

Introduction—Osteogenesis imperfecta is a heritable connective tissue disorder due primarily to mutations in the type I collagen genes resulting in skeletal deformity and fragility. Currently, there is no cure, and therapeutic strategies encompass the use of antiresorptive pharmaceuticals and surgical bracing, with limited success and significant potential for adverse effects. Bone, a mechanosensing organ, can respond to high mechanical loads by increasing new bone formation and altering bone geometry to withstand increased forces. Skeletal muscle is a major source of physiological loading on bone, and bone strength is proportional to muscle mass.

Methods—To test the hypothesis that congenic increases in muscle mass in the osteogenesis imperfecta murine model mouse (*oim*) will improve their compromised bone quality and strength, heterozygous (+/*oim*) mice were bred to mice deficient in myostatin (+/*mstn*), a negative regulator

of muscle growth. The resulting adult offspring were evaluated for hindlimb muscle mass, and bone microarchitecture, physiochemistry, and biomechanical integrity.

Results—+/*oim* mice deficient in myostatin (+/*mstn* +/*oim*) were generated and demonstrated that myostatin deficiency increased body weight, muscle mass, and biomechanical strength in +/*mstn* +/*oim* mice as compared to +/*oim* mice. Additionally, myostatin deficiency altered the physiochemical properties of the +/*oim* bone but did not alter bone remodeling.

Conclusions—Myostatin deficiency partially improved the reduced femoral bone biomechanical strength of adult +/*oim* mice by increasing muscle mass with concomitant improvements in bone microarchitecture and physiochemical properties.

Introduction

Osteogenesis imperfecta (OI) is a genetically and clinically heterogeneous heritable connective tissue disorder characterized by anomalies in type I collagen-containing tissues such as bone [1, 2]. The major structural protein comprising the organic component of bone is type I collagen. More than 1000 distinct OI-causing mutations have been identified with 90 % of OI causing mutations in one of the two procollagen genes, COL1A1 and COL1A2 [1, 2]. Individuals with OI exhibit a broad range of clinical outcomes and manifestations including osteopenia with fractures, skeletal deformities, short stature, and skeletal muscle weakness [1–3]. The osteogenesis imperfecta murine model (*oim*/*oim*) mice are homozygous for a functional null mutation in the *Col1a2* gene of type I collagen [4]. *Oim*/*oim* mice have a similar phenotype to human patients with moderately severe OI, including reduced bone biomechanical integrity and bone mineral density as well as altered bone mineral composition and inherent skeletal muscle weakness [4–7]. The heterozygous (+/*oim*) mice carry a single mutant *Col1a2* allele and synthesize both homotrimeric and heterotrimeric type I collagen. +/*oim* mice model the milder clinical severity of human type I OI individuals. While fractures are less frequent in +/*oim* mice compared to homozygous *oim*/*oim* mice, the +/*oim* mice still exhibit altered midshaft geometry, decreased biomechanical strength, collagen content, crystallinity, and crack-initiation toughness when compared to wild-type (Wt) littermates, though to a lesser degree than *oim*/*oim* [6, 8–10]. Current treatment strategies for OI patients primarily target symptoms, not the underlying cause of the disease, and are limited to pharmacologic use of antiresorptive drugs and surgical interventions to brace the bone. Both approaches have limited success and significant concerns due to frequency of failure and potential side effects of long-term use [2].

The skeleton is a mechanosensing organ, responding and adapting to its mechanical environment [11, 12]. Bone formation occurs in response to high mechanical loads, often changing the geometry to strengthen the skeleton [11–14]. Some of the largest physiological loads bones experience are from muscle, with bone strength proportional to muscle mass [12]. We postulated that although the OI bone material is bio-mechanically weaker, the bone

will be able to respond to increased muscle mass, especially during pubertal growth, by altering bone geometry, architecture, material properties, and/or mass to generate an inherently stronger bone.

Myostatin is a negative regulator of muscle growth and a transforming growth factor-beta (TGF-β) family member. In homozygous myostatin mice (*mstn/mstn*), myostatin is developmentally absent, and the result is significantly greater muscle mass due to muscle hyperplasia and hypertrophy [15, 16]. Heterozygous (+/*mstn*) mice have an intermediate phenotype as compared to Wt and *mstn/mstn*, suggesting a dose effect of the myostatin protein [17]. Partial myostatin inhibition as seen in +/*mstn* mice and in whippet dogs heterozygous for a myostatin mutation results in increased muscle size and function with minimal lesions [17, 18]. In addition to the increased muscle mass, *mstn/mstn* mice exhibit altered bone geometry [19] and display a concomitant increase in bone strength [14].

We hypothesized that although *oim* muscle and bone are compromised, a reduction in myostatin protein levels during fetal development and throughout life would increase muscle mass and mechanical load in +/*oim* mice causing the bone to respond by altering bone geometry, microarchitecture, physiochemical properties, and/or mass to generate an inherently stronger bone and attenuate the bone phenotype of +/*oim* mice. Our findings demonstrate that partial myostatin deficiency (+/*mstn*) results in increased muscle mass and moderate improvements in femoral bone quality and strength in +/*oim* mice by primarily impacting the bone microarchitecture and physiochemical composition rather than cortical bone geometry.

Materials and methods

Animals

To determine the impact of myostatin deficiency in the presence of the +/*oim* mutation, both mouse models, *mstn* and *oim*, were bred and maintained on a congenic C57BL/6J (Jackson Laboratory, Bar Harbor, Maine) background to control for potential modifier gene effects. Mice were housed in an AAALAC accredited facility at the University of Missouri-Columbia and had ad libitum access to water and food (Purina 5008 Formulab Diet; Purina Mills Inc., St Louis, MO). The protocols used for this study were performed under an approved University of Missouri Animal Care and Use Protocol. Dams heterozygous for myostatin deficiency (+/*mstn*) were bred to sires heterozygous for the *oim* mutation (+/*oim*) (Fig. 1A). The offspring were raised to 4 months of age (peak bone mineral density [20]), sacrificed, and their serum, hindlimb muscles, tibiae, and femora harvested for analyses.

Tissue harvest

Left hindlimb muscles (soleus, plantaris, gastrocnemius, tibialis anterior, and quadriceps) were removed, cleaned of extraneous tissue, blotted, and weighed. Femora and tibiae were excised, the soft tissue removed, and the bones wrapped in sterile gauze soaked in sterile 1× phosphate-buffered saline (PBS) prior to storage at −20 °C.

Tibial microarchitecture analyses

Prior to analyses by Raman spectroscopy, the macroarchitecture and microarchitecture of the left tibiae were determined by microcomputed tomography (μCT) with the vivaCT 40 (Scanco Medical AG, Bassersdorf, Switzerland) as previously described [9] using 55-kVp X-ray tube potential, 145-μA current, 10-μm voxel resolution, and 200-ms integration time to assess cortical bone and trabecular bone properties. By hydroxyapatite calibration, the voxel values were converted to a mineral-equivalent value, milligrams per cubic centimeter (mg/cm^3). Three-dimensional images of the tibiae were reconstructed along the long axis with series of 10-μm-thick slices, using a global threshold of 253 (μCT gray value). For each tibia, the proximal metaphysic trabecular bone was analyzed 1 mm below the growth plate, while the cortical bone was evaluated at the mid-shaft starting 1 mm above fibula-tibia junction.

Femoral μCT and torsional loading to failure

The geometric parameters of the right femora were determined by μCT analyses (MicroCAT II, Siemens Medical), and the image slices reconstructed using the Amira 5.3.3 software package (Mercury Computer Systems/TGS, Chelmsford, MA) to give a cubic voxel dimension of $0.083 mm^3$ as previously described [21]. Each femora was then subjected to torsional loading to failure analyses to determine the mechanical properties of the whole bone and the bone material using the TA-HDi testing machine (Stable Micro Systems, Surrey, UK) as previously described [21]. Applied torque T (Nmm) was determined and evaluated as a function of relative angular displacement θ (degrees) (Fig. 1B). Torsional ultimate strength (T_{max}, Nmm), strain energy to failure (U, Nmm), and stiffness (torsional stiffness, Nmm/rad) are whole bone parameters reflecting the contributions of both the bone geometry and the bone material properties. The bone material properties, tensile strength (Su, N/mm^2), and shear modulus of elasticity (N/mm^2) are independent of bone size and shape [21].

Bone mineral and matrix composition

Left tibial cortical bone cross sections were evaluated by Raman spectroscopy using a LabRam HR 800 Raman spectrometer (Horiba JobinYvon, Edison, NJ). Average bone biochemical composition was determined from Raman spectra (700- to 1800-cm^{-1} range) that were excited by a helium-neon laser (633 nm) with a 20× water immersion objective as previously described [9], allowing acquisition of peaks attributed to the bone minerals and proteins. Each tibia was examined at 4 points from anterior, posterior, medial, and lateral cross section and the data averaged for each sample. Spectral analyses were performed to measure the area of hydroxyapatite phosphate (ν_1 PO_4^{3-}; 960 cm^{-1}), carbonate (type B ν_1 CO_3^{2-}; 1070 cm^{-1}), matrix (CH_2; 1450 cm^{-1}), and collagen (amide I; 1640 cm^{-1}) bands [9]. Assessed were as follows: (1) the phosphate/CH_2 ratio, which increases with increasing bone mineral content; (2) the phosphate/carbonate, which decreases with increasing bone age; and (3) the PO_4/amide I ratio, which represents the bone mineral to collagen ratio [22].

To quantitate bone collagen, the left femora were weighed and the collagen content determined indirectly by quantitation of hydroxyproline content (μg/g bone) as described by Stegemann and Stalder [23].

Serum biomarkers of collagen synthesis and degradation

At the time of sacrifice, blood was collected by exsanguination and the serum separated by centrifugation at 14,000 rpm for 15 min and stored at −80 °C until assayed. Serum levels of N-terminal propeptide of type I procollagen (PINP), a biomarker of collagen synthesis, and C-terminal cross-linked telopeptide of type I collagen (CTX), a biomarker of collagen degradation, were quantitated using the commercially available enzyme immunoassay kits, the Rat/Mouse PINP EIA kit (AC-33F1) and the RatLaps™ EIA kit (AC-06F1) by Immunodiagnostics Systems (Scottsdale, Arizona), respectively. Samples and standards were assayed in duplicate following the manufacturer's specifications except that the microplate was placed on a shaker at 400 rpm rather than the suggested 500–700 rpm. The samples and standards were measured at A_{450} and A_{650} using the BioTek Synergy 2 Multi-Mode Reader and Gen5™ Data Analysis Software v2.00.17 (Winooski, Vermont). A standard curve was generated by plotting the absorbance and concentration values of the standards using a four parameter logistic curve-fit.

Statistical analysis

Statistical analyses were performed using SAS (SAS Institute Inc., Cary, NC). Data were analyzed as a 4×2 factorial arrangement [4 genotypes and 2 sexes]. Specifically, the body, muscle, and relative muscle weights were evaluated by analysis of variance, and the bone geometric and biomechanical parameters, hydroxyproline content, and Raman spectroscopy physiochemical ratios, as well as the serum PINP and CTX data, were evaluated by analysis of covariance with body weight as the covariate. Genotype and sex interactions and the genotype and sex main effects were evaluated. Genotype and sex interactions were significant for only two of the parameters evaluated, the tibial trabecular thickness and separation. Body, muscle and relative muscle weights, and bone geometric and biomechanical parameters, hydroxyproline content, serum biomarkers, and physiochemical ratios all exhibited a main genotype effect, allowing pooling of male and female values. The main genotype effect values for the parameters are presented as the LSmeans±SE. When heterogeneous variations made it necessary, a log transformation was used to stabilize the variation. If the log transformation failed to stabilize the variation, a nonparametric ranked analysis was performed according to Conover et al. [25]. Mean differences were determined using Fisher's protected least significant difference (LSD) (24). Differences were considered to be significant at p 0.05.

Results

Body and muscle weights

To assess the effect of the myostatin deficiency on the body and hindlimb muscle weights of +/*oim* mice, Wt, +/*mstn*, +/*mstn* +/*oim*, and +/*oim* mice were sacrificed, weighed, and their muscles harvested. Wt, +/*mstn*, and +/*mstn* +/*oim* mice weighed more than +/*oim* mice, with +/*mstn* +/*oim* mice weighing 11 % more than their +/*oim* littermates. +/*mstn* and +/*mstn* +/*oim* mice had greater muscle weights for all five hindlimb muscles relative to their Wt and +/*oim* littermates (Table 1). Even when muscle weight was normalized to the body weight, the relative muscle weights of +/*mstn* mice remained greater than Wt, while the +/*oim* mice relative muscle weights were not significantly different from Wt mice. The relative muscle

weights of +/*mstn* and +/*mstn* +/*oim* were equivalent, and +/*mstn* +/*oim* relative muscle weights were also greater than Wt, reaching significance for the plantaris and tibialis anterior muscles.

Tibial microarchitecture

Wt, +/*mstn*, +/*mstn* +/*oim*, and +/*oim* mouse tibiae were evaluated by μCT analyses and demonstrated that +/*mstn* tibiae had increased trabecular bone volume fraction (BV/TV), trabecular number, and connectivity density, along with decreased trabecular density, structure model index (SMI), and cortical density compared to Wt tibiae (Table 2). The deficiency of myostatin in the +/*mstn* +/*oim* tibia decreased trabecular and cortical bone densities and increased connectivity density of the +/*oim* bone. Myostatin deficiency improved the +/*oim* bone so that trabecular number and connectivity density in the +/*mstn* +/*oim* bone were no longer different from Wt (Table 2). Analysis of the trabecular thickness and trabecular separation revealed a sex and genotype interaction, indicating that males and females responded differently to myostatin deficiency. Myostatin deficiency increased trabecular thickness in male +/*mstn* and +/*mstn* +/*oim* tibiae relative to Wt and +/*oim* but did not impact female tibial trabecular thickness (Table 2). Trabecular separation was decreased by 8 % in female +/*mstn* +/*oim* tibiae compared to female +/*oim* tibiae, and by 5 % in male +/*mstn* +/*oim* tibiae compared to male +/*oim*, although it did not reach significance in males (Table 2).

Femoral geometry

The femoral geometry of male and female Wt, +/*mstn*, +/*mstn* +/*oim*, and +/*oim* mice was also assessed by μCT analyses prior to torsional loading to failure. Femoral length and cortical bone width were equivalent across all genotypes. Cortical bone measurements at the midshaft slice were used to calculate polar moment of inertia, a geometric parameter which predicts an object's ability to resist torsion; the greater the polar moment of inertia, the greater the predicted resistance to torque. Wt and +/*mstn* femora had equivalent polar moment of inertia and marrow cavity diameters, which were greater than the polar moment of inertia and marrow cavity diameters of the +/*mstn* +/*oim* and +/*oim* femora. Femora from +/*mstn* +/*oim* and +/*oim* mice did not exhibit differences in femoral geometry for all the parameters tested (Table 3).

Femoral biomechanics

To evaluate bone biomechanical integrity, femora from Wt, +/*mstn*, +/*mstn* +/*oim*, and +/*oim* mice were analyzed by torsional loading to failure [21]. The torsional ultimate strength (T_{max}), a whole bone property measuring the maximum force required to break the bone, of +/*mstn* +/*oim* femora displayed a 25 % improvement relative to +/*oim* femora although the improvement did not reach significance (Fig. 1C). The decreased levels of myostatin in the +/*mstn* +/*oim* mouse improved the tensile strength, a measure of the bone material, by 22 %, and although the difference did not reach significance, the improvement increased +/*mstn* +/*oim* tensile strength to that of Wt femora (Fig. 1D). The whole bone parameter, energy to failure had increased 63 % in the +/*mstn* +/*oim* compared to +/*oim* mouse femora and was now equivalent to both Wt and +/*mstn* femora (Fig. 1E), further suggesting that myostatin deficiency in the +/*mstn* +/*oim* enabled the bone to absorb more energy before fracturing.

The femoral stiffness of $+/mstn$ $+/oim$ and $+/oim$ mice was equivalent (Fig. 1F), and the shear modulus of elasticity of the femora, the measure of the stiffness of the bone material, was equivalent among femora from all genotypes examined (Fig. 1G).

Mineral-matrix interactions and collagen content

Bone is composed of an organic component, primarily type I collagen, and a mineral component, hydroxyapatite crystals. The ability of bone to resist fracture depends on bone mass and geometry as well as the intrinsic physiochemical properties and microarchitecture of the bone material. To investigate the composition and quality of the bone material, we examined the mineral and matrix composition using Raman spectroscopy (Fig. 2). Genotype differences were not observed in PO_4/CO_3 (phosphate to carbonate) ratios among Wt, $+/mstn$, $+/mstn$ $+/oim$, and $+/oim$ tibiae (Fig. 2A). Tibiae from $+/mstn$ $+/oim$ and $+/oim$ had equivalent PO_4/CH_2 (mineral to protein) ratios, which were both increased by 12 % compared to Wt and $+/mstn$ tibiae (Fig. 2B). The PO_4/amide I (mineral to collagen) ratio of $+/oim$ tibiae was greater than the PO_4/amide I ratio of Wt tibiae (Fig. 2C). The presence of the myostatin mutation in the $+/mstn$ $+/oim$ reduced the PO_4/amide I ratio compared to $+/oim$ tibiae, making the PO_4/amide I ratio of $+/mstn$ $+/oim$ tibiae equivalent to tibiae of Wt littermates (Fig. 2C).

To evaluate if the increased PO_4/CH_2 and PO_4/amide I ratios in $+/oim$ bone reflects decreases in the organic component, collagen, or increases in mineral component, hydroxyapatite, we examined collagen content indirectly by quantification of the hydroxyproline content (Fig. 2D). Wt and $+/mstn$ femora had equivalent hydroxyproline levels. Femora from both $+/mstn$ $+/oim$ and $+/oim$ contained 10 and 16 % less hydroxyproline per bone weight than Wt femora, respectively, suggesting that myostatin deficiency did not significantly alter femoral collagen content of the femora (Fig. 2D).

Biochemical markers of bone remodeling

To begin to discern if differences in Wt, $+/mstn$, $+/mstn$ $+/oim$, and $+/oim$ bone material and physiochemical properties were associated with changes in bone remodeling, serum biochemical markers of bone turnover were evaluated [24]. Serum PINP (a marker of bone formation) concentrations were similar in mice from all genotypes examined, suggesting that myostatin deficiency did not significantly impact bone formation (Fig. 3A). Serum CTX (a marker of bone resorption) concentrations indicated that $+/mstn$ $+/oim$ and $+/oim$ mice had similar levels of serum CTX, which were approximately 6-fold greater than serum CTX levels in Wt and $+/mstn$ mice (Fig. 3B). While myostatin deficiency increased CTX levels in the $+/mstn$ mice compared to Wt (Fig. 3B), the elevated serum CTX levels in $+/mstn$ $+/oim$ suggest that myostatin deficiency was not able to attenuate the elevated osteoclast activity present in the $+/oim$ mouse.

Discussion

Our findings demonstrated that myostatin deficiency throughout development and maturation in the $+/oim$ mouse resulted in increased body and muscle weights, with a concomitant enhancement of bone physiochemical properties and strength in the $+/oim$

mouse. Myostatin deficiency was anticipated to increase +/*oim* body weight and muscle mass of each of the hindlimb muscles tested, as was previously seen in myostatin deficient and knockout mice [16, 17, 25]. We demonstrate that the increased hindlimb muscle mass persists in the presence of the *oim* mutation. The increase in muscle mass corresponded to increases in trabecular microarchitecture, femoral strength, and modest alterations in the bone physiochemical properties. Yet, the increase in muscle mass in +/*mstn* +/*oim* mice did not translate into significant changes in midshaft bone geometry. This was consistent with observations that *mstn*/*mstn* mice exhibit long bone changes that are primarily localized to the sites of muscle insertion, and the impact of heterozygosity (+/*mstn*) at the *mstn* locus on bone appears more subtle [19, 26].

To determine if the observed improvements in the bone of +/*mstn* +/*oim* mice were due to their increased body size relative to the +/*oim* littermates, we analyzed our data using an analysis of covariance, with body weight as the covariate. Our analyses indicated that the improvements in tibial microarchitecture, geometry, and biomechanical strength seen in +/*mstn* +/*oim* mice could not be accounted for simply by the increase in body weight of +/*mstn* +/*oim* mice relative to +/*oim* mice. Our analysis also indicated that body mass differences did not account for the main sex effect which was evident for nearly all the parameters evaluated (data not shown).

Tibiae from +/*mstn* +/*oim* mice showed modest changes in microarchitecture compared to +/*oim* mouse tibiae, including increases in trabecular number and connectivity densities. The decreases in +/*mstn* +/*oim* bone densities suggest that myostatin deficiency either decreased mineral acquisition or increased collagen deposition in the +/*oim* mouse bone, with the decreased density hypothesized to reduce brittleness. We did not see an increase in the cortical bone width in +/*mstn* femora, as had been previously reported in *mstn*/*mstn* mice [27], which may reflect a dose effect of partial (heterozygous) myostatin deficiency versus complete (homozygous) absence of myostatin. The hydroxyproline content of the +/*mstn* +/*oim* bone was 7 % greater than the +/*oim* bone; although this increase did not reach significance, it may contribute partially to the +/*mstn* +/*oim* bone having decreased PO_4/amide I ratios and increased tensile strength relative to +/*oim* bone.

Increased +/*mstn* +/*oim* femoral energy to failure demonstrated that myostatin deficiency was able to enhance +/*oim* femoral biomechanical integrity such that the +/*mstn* +/*oim* femora were no longer significantly weaker than Wt femora, thus demonstrating that myostatin deficiency partially rescued the +/*oim* bone phenotype. The femoral torsional ultimate strength, T_{max}, was also increased in +/*mstn* +/*oim* mice compared to their +/*oim* littermates, though this trend (*p*=0.098) did not reach significance. These data demonstrated that the femora of +/*oim* mice exhibit improvements in bone biomechanical integrity when the mice were deficient in myostatin throughout their lifetime.

Evaluation of serum markers of bone turnover indicated that bone resorption was increased in mice with the +/*oim* mutation without significant impact on bone formation and that this difference remains despite the presence of the +/*mstn* mutation. The increase in serum CTX associated with +/*oim* and +/*mstn* +/*oim* is consistent with studies demonstrating that *oim*/*oim* mice have increased osteoclast numbers and resorptive activity [28], as well as with the

findings in other mouse models of OI, *Brtl* [29] and *Col1a1*^{Jrt}/+ [30]. In vitro studies suggested that *oim*/*oim* mice have impaired osteogenesis and failure to reach the terminal stage of maturation [31]. Mesenchymal stem cells from the *Brtl* OI mouse model (glycine to cysteine substitution in the *Col1a1* gene) also exhibited reduced osteogenic potential, which was attributed in part to autophagy activation [32]. The serum PINP findings suggest that myostatin deficiency did not appear to alter bone formation. The impact of myostatin deficiency on osteoblast maturation and differentiation remains to be further elucidated.

The impact of myostatin deficiency on the bone biomechanical and physiochemical properties suggests that myostatin levels may also alter the bone matrix and potentially its architectural organization rather than simply altering bone shape. In a previous study, we demonstrated by Raman spectroscopy that there were no sex-related differences in PO_4/CO_3, PO_4/CH_2, and PO_4/amide I ratios between Wt, +/*oim*, and *oim*/*oim* tibias, but that there were significant genotype-related differences [9]. *Oim*/*oim* bone was found to have significantly higher PO_4/CO_3 and PO_4/CH_2 ratio relative to Wt bone, with +/*oim* bone having intermediate values [9]. Tibiae from +/*mstn* +/*oim* and +/*oim* maintained PO_4/CH_2 ratios greater than those from Wt (Fig. 2B) suggesting that the skeletal mineral to protein ratio is more strongly impacted by the collagen status than myostatin levels. The PO_4/CO_3 ratio changes as the bone tissue ages, with the PO_4/CO_3 ratio decreasing with increasing age. Previous studies suggested that the *oim*/*oim* tibial mineralized matrix had not matured to the same extent as their age-matched Wt littermates [9]. The increased PO_4/CH_2, mineral to matrix ratios, in *oim* mice has been attributed to reduced collagen content and hypermineralization. Hypermineralization in the *oim* mouse and in other mouse models of OI has previously been reported [6, 21, 33, 34] and correlated to increased brittleness [9, 32, 33]. Tibiae from +/*mstn* +/*oim* mice showed a decrease in cortical and trabecular bone densities (Table 2) compared to +/*oim*, which was consistent with myostatin deficiency resulting in decreased PO_4/amide I ratios.

While it is well established that bone and muscle are functionally dependent upon the shared forces of the mechanostat unit, our growing knowledge of the musculoskeletal system has led us to the understanding that both bone and muscle can interact through secreted factors as well. A growing amount of data suggests that muscle and bone can signal in a paracrine and endocrine fashion through secreted factors such as myokines and osteokines (for review [35]). Myostatin is a growth factor produced primarily by muscle, secreted into the circulation, and is a candidate for bone-muscle crosstalk as it has been shown to decrease osteogenic differentiation of bone marrow-derived mesenchymal stem cells [36]. Myostatin has also been shown to be localized to sites of musculoskeletal injury [37], and the loss or inhibition of myostatin is known to have an osteogenic effect [36] and improve fracture healing [38] in mouse models. While it is likely that the deficiency of myostatin in an OI mouse model may be working to improve the bone by increasing muscle size and the mechanical stimuli the bone is exposed to, it is also reasonable to speculate that the decrease of myostatin may also have a direct osteogenic effect. Although serum PINP and CTX markers of bone remodeling were not altered by myostatin deficiency in the OI mouse, additional histomorphometric analyses to examine osteoblast number and activity, as well as expression studies to evaluate potential myostatin target genes and intracellular signaling

pathways, are necessary to begin to elucidate the mechanism by which myostatin impacts OI bone.

From these results, one might postulate that complete absence of myostatin (*mstn/mstn*) in homozygous *oim/oim* mice would exhibit a dramatic positive response in muscle and bone. Myostatin is a member of the TGF-β superfamily of growth regulators, and TGF-β is a known positive regulator of collagen and has been implicated in fibrosis [39–41]. Myostatin has been shown to directly affect skeletal muscle fibrosis by inducing muscle fibroblast proliferation [42]. Consistent with these observations is that myostatin deficient mice have less collagen in their muscles and fail to accumulate increased connective tissue in muscles as they age [43]. In addition, *mstn/mstn* mice exhibit compromised muscle function [17] and are reported to have brittle tendons with reduced collagen content [44]. Given the association of myostatin in collagen expression, we targeted partial deficiency of myostatin, as complete absence of myostatin in the presence of the already compromised muscle function [7] and collagen of *oim/oim* tendon [45] would likely have been detrimental. Tendons are the conduit through which muscle loading transduces the mechanosignal to the bone. Myostatin deficiency may not only indirectly impact bone by altering muscle loading, but the mechanosignaling between the muscle and bone via the tendon may be altered as well. Alterations in tendon material properties could alter the mechanosignal transduction of the load to the bone and should be investigated further.

Increasing our understanding of the role of myostatin in regulatory mechanisms of collagen expression, mineralization, and bone strength will provide unique insight and promote potential new therapeutic approaches to enhancing and protecting bone health. Our results suggest that intervention of the myostatin signaling pathway by potential pharmacological agents holds promise as a therapeutic strategy for individuals with osteogenesis imperfecta by not only enhancing muscle function, but also bone strength. The use of myostatin inhibitors or receptor decoy molecules in normal mice and mice with acquired bone loss has resulted in increased muscle mass, increased serum bone formation markers, bone mineral density, and bone mass [46, 47]. These studies together with our findings demonstrate the need to further elucidate the mechanisms of action of myostatin signaling on bone and suggest that pharmacological inhibition of myostatin signaling may offer new therapeutic strategies to enhance muscle and bone strength in individuals with osteogenesis imperfecta.

Acknowledgments

References

1. Van Dijk FS, Sillence DO (2014) Osteogenesis imperfecta: clinical diagnosis, nomenclature and severity assessment. Am J Med Genet A 164:1470–1481

2. Cundy T (2012) Recent advances in osteogenesis imperfecta. Calcif Tissue Int 90:439–449 [PubMed: 22451222]

3. Veilleux LN, Lemay M, Pouliot-Laforte A, Cheung MS, Glorieux FH, Rauch F (2014) Muscle anatomy and dynamic muscle function in osteogenesis imperfecta type I. J Clin Endocrinol Metab 99: E356–E362 [PubMed: 24248189]

4. Chipman SD, Sweet HO, McBride DJ Jr, Davisson MT, Marks SC Jr, Shuldiner AR, Wenstrup RJ, Rowe DW, Shapiro JR (1993) Defective pro alpha 2(I) collagen synthesis in a recessive mutation in mice: a model of human osteogenesis imperfecta. Proc Natl Acad Sci U S A 90:1701–1705 [PubMed: 8446583]

5. McBride DJ Jr, Shapiro JR, Dunn MG (1998) Bone geometry and strength measurements in aging mice with the oim mutation. Calcif Tissue Int 62:172–176 [PubMed: 9437052]

6. Camacho NP, Hou L, Toledano TR, Ilg WA, Brayton CF, Raggio CL, Root L, Boskey AL (1999) The material basis for reduced mechanical properties in oim mice bones. J Bone Miner Res 14: 264–272 [PubMed: 9933481]

7. Gentry BA, Ferreira JA, McCambridge AJ, Brown M, Phillips CL (2010) Skeletal muscle weakness in osteogenesis imperfecta mice. Matrix Biol 29:638–644 [PubMed: 20619344]

8. Saban J, Zussman MA, Havey R, Patwardhan AG, Schneider GB, King D (1996) Heterozygous oim mice exhibit a mild form of osteogenesis imperfecta. Bone 19:575–579 [PubMed: 8968022]

9. Yao X, Carleton SM, Kettle AD, Melander J, Phillips CL, Wang Y (2013) Gender-dependence of bone structure and properties in adult osteogenesis imperfecta murine model. Ann Biomed Eng 41:1139–1149 [PubMed: 23536112]

10. Carriero A, Zimmermann EA, Paluszny A, Tang SY, Bale H, Busse B, Alliston T, Kazakia G, Ritchie RO, Shefelbine SJ (2014) How tough is brittle bone? investigating osteogenesis imperfecta in mouse bone. J Bone Miner Res 29:1392–1401 [PubMed: 24420672]

11. Warden SJ, Hurst JA, Sanders MS, Turner CH, Burr DB, Li J (2005) Bone adaptation to a mechanical loading program significantly increases skeletal fatigue resistance. J Bone Miner Res 20: 809–816 [PubMed: 15824854]

12. Turner CH (2006) Bone strength: current concepts. Ann N Y Acad Sci 1068:429–446 [PubMed: 16831941]

13. Kodama Y, Umemura Y, Nagasawa S, Beamer WG, Donahue LR, Rosen CR, Baylink DJ, Farley JR (2000) Exercise and mechanical loading increase periosteal bone formation and whole bone strength in C57BL/6J mice but not in C3H/Hej mice. Calcif Tissue Int 66: 298–306 [PubMed: 10742449]

14. Hamrick MW, Samaddar T, Pennington C, McCormick J (2006) Increased muscle mass with myostatin deficiency improves gains in bone strength with exercise. J Bone Miner Res 21:477–483 [PubMed: 16491296]

15. Kollias HD, McDermott JC (2008) Transforming growth factor-beta and myostatin signaling in skeletal muscle. J Appl Physiol 104:579–587 [PubMed: 18032576]

16. McPherron AC, Lawler AM, Lee SJ (1997) Regulation of skeletal muscle mass in mice by a new TGF-beta superfamily member. Nature 387:83–90 [PubMed: 9139826]

17. Gentry BA, Ferreira JA, Phillips CL, Brown M (2011) Hindlimb skeletal muscle function in myostatin-deficient mice. Muscle Nerve 43:49–57 [PubMed: 21082689]

18. Mosher DS, Quignon P, Bustamante CD, Sutter NB, Mellersh CS, Parker HG, Ostrander EA (2007) A mutation in the myostatin gene increases muscle mass and enhances racing performance in heterozygote dogs. PLoS Genet 3:e79 [PubMed: 17530926]

19. Elkasrawy MN, Hamrick MW (2010) Myostatin (GDF-8) as a key factor linking muscle mass and bone structure. J Musculoskelet Neuronal Interact 10:56–63 [PubMed: 20190380]

20. Beamer WG, Shultz KL, Donahue LR, Churchill GA, Sen S, Wergedal JR, Baylink DJ, Rosen CJ (2001) Quantitative trait loci for femoral and lumbar vertebral bone mineral density in C57BL/6J and C3H/HeJ inbred strains of mice. J Bone Miner Res 16:1195–1206 [PubMed: 11450694]

21. Carleton SM, McBride DJ, Carson WL, Huntington CE, Twenter KL, Rolwes KM, Winkelmann CT, Morris JS, Taylor JF, Phillips CL (2008) Role of genetic background in determining phenotypic severity throughout postnatal development and at peak bone mass in Col1a2 deficient mice (oim). Bone 42:681–694 [PubMed: 18313376]

22. Mandair GS, Morris MD (2015) Contributions of Raman spectroscopy to the understanding of bone strength. BoneKEy Rep 4

23. Stegemann H, Stalder K (1967) Determination of hydroxyproline. Clin Chim Acta 18:267–273 [PubMed: 4864804]

24. Naylor K, Eastell R (2012) Bone turnover markers: use in osteoporosis. Nat Rev Rheumatol 8:379–389 [PubMed: 22664836]

25. Lee SJ (2007) Quadrupling muscle mass in mice by targeting TGF-beta signaling pathways. PLoS One 2:e789 [PubMed: 17726519]

26. Hamrick MW, McPherron AC, Lovejoy CO (2002) Bone mineral content and density in the humerus of adult myostatin-deficient mice. Calcif Tissue Int 71:63–68 [PubMed: 12060865]

27. Hamrick MW (2003) Increased bone mineral density in the femora of GDF8 knockout mice. Anat Rec A: Discov Mol Cell Evol Biol 272:388–391

28. Zhang H, Doty SB, Hughes C, Dempster D, Camacho NP (2007) Increased resorptive activity and accompanying morphological alterations in osteoclasts derived from the oim/oim mouse model of osteogenesis imperfecta. J Cell Biochem 102:1011–1020 [PubMed: 17668424]

29. Uveges TE, Collin-Osdoby P, Cabral WA, Ledgard F, Goldberg L, Bergwitz C, Forlino A, Osdoby P, Gronowicz GA, Marini JC (2008) Cellular mechanism of decreased bone in Brtl mouse model of OI: imbalance of decreased osteoblast function and increased osteoclasts and their precursors. J Bone Miner Res 23:1983–1994 [PubMed: 18684089]

30. Chen F, Guo R, Itoh S et al. (2014) First mouse model for combined osteogenesis imperfecta and Ehlers-Danlos syndrome. J Bone Miner Res 29:1412–1423 [PubMed: 24443344]

31. Li H, Jiang X, Delaney J, Franceschetti T, Bilic-Curcic I, Kalinovsky J, Lorenzo JA, Grcevic D, Rowe DW, Kalajzic I (2010) Immature osteoblast lineage cells increase osteoclastogenesis in osteogenesis imperfecta murine. Am J Pathol 176:2405–2413 [PubMed: 20348238]

32. Gioia R, Panaroni C, Besio R et al. (2012) Impaired osteoblastogenesis in a murine model of dominant osteogenesis imperfecta: a new target for osteogenesis imperfecta pharmacological therapy. Stem Cells 30:1465–1476 [PubMed: 22511244]

33. Coleman RM, Aguilera L, Quinones L, Lukashova L, Poirier C, Boskey A (2012) Comparison of bone tissue properties in mouse models with collagenous and non-collagenous genetic mutations using FTIRI. Bone 51:920–928 [PubMed: 22910579]

34. Camacho NP, Landis WJ, Boskey AL (1996) Mineral changes in a mouse model of osteogenesis imperfecta detected by Fourier transform infrared microscopy. Connect Tissue Res 35:259–265 [PubMed: 9084664]

35. Brotto M, Johnson ML (2014) Endocrine crosstalk between muscle and bone. Curr Osteop Rep 12:135–141

36. Hamrick MW, Shi X, Zhang W, Pennington C, Thakore H, Haque M, Kang B, Isales CM, Fulzele S, Wenger KH (2007) Loss of myostatin (GDF8) function increases osteogenic differentiation of bone marrow-derived mesenchymal stem cells but the osteogenic effect is ablated with unloading. Bone 40:1544–1553 [PubMed: 17383950]

37. Elkasrawy M, Immel D, Wen X, Liu X, Liang LF, Hamrick MW (2012) Immunolocalization of myostatin (GDF-8) following musculoskeletal injury and the effects of exogenous myostatin on muscle and bone healing. J Histochem Cytochem : Off J Histochem Soc 60:22–30

38. Hamrick MW, Arounleut P, Kellum E, Cain M, Immel D, Liang LF (2010) Recombinant myostatin (GDF-8) propeptide enhances the repair and regeneration of both muscle and bone in a model of deep penetrant musculoskeletal injury. J Trauma 69:579–583 [PubMed: 20173658]

39. Verrecchia F, Mauviel A (2004) TGF-beta and TNF-alpha: antagonistic cytokines controlling type I collagen gene expression. Cell Signal 16:873–880 [PubMed: 15157666]

40. Ghosh AK (2002) Factors involved in the regulation of type I collagen gene expression: implication in fibrosis. Exp Biol Med (Maywood) 227:301–314 [PubMed: 11976400]

41. Hosaka YZ, Ishibashi M, Wakamatsu J, Uehara M, Nishimura T (2012) Myostatin regulates proliferation and extracellular matrix mRNA expression in NIH3T3 fibroblasts. Biomed Res 33:355–361 [PubMed: 23268959]

42. Li ZB, Kollias HD, Wagner KR (2008) Myostatin directly regulates skeletal muscle fibrosis. J Biol Chem 283:19371–19378 [PubMed: 18453534]

43. Elashry MI, Collins-Hooper H, Vaiyapuri S, Patel K (2012) Characterisation of connective tissue from the hypertrophic skeletal muscle of myostatin null mice. J Anat 220:603–611 [PubMed: 22463481]

44. Mendias CL, Bakhurin KI, Faulkner JA (2008) Tendons of myostatin-deficient mice are small, brittle, and hypocellular. Proc Natl Acad Sci U S A 105:388–393 [PubMed: 18162552]

45. McBride DJ Jr, Choe V, Shapiro JR, Brodsky B (1997) Altered collagen structure in mouse tail tendon lacking the alpha 2(I) chain. J Mol Biol 270:275–284 [PubMed: 9236128]

46. Chiu CS, Peekhaus N, Weber H, et al. (2013) Increased muscle force production and bone mineral density in ActRIIB-Fc-treated mature rodents. J Gerontol A Biol Sci Med Sci

47. Bialek P, Parkington J, Li X et al. (2014) A myostatin and activin decoy receptor enhances bone formation in mice. Bone 60:162–171 [PubMed: 24333131]

Author Manuscript

Author Manuscript

Author Manuscript

Author Manuscript
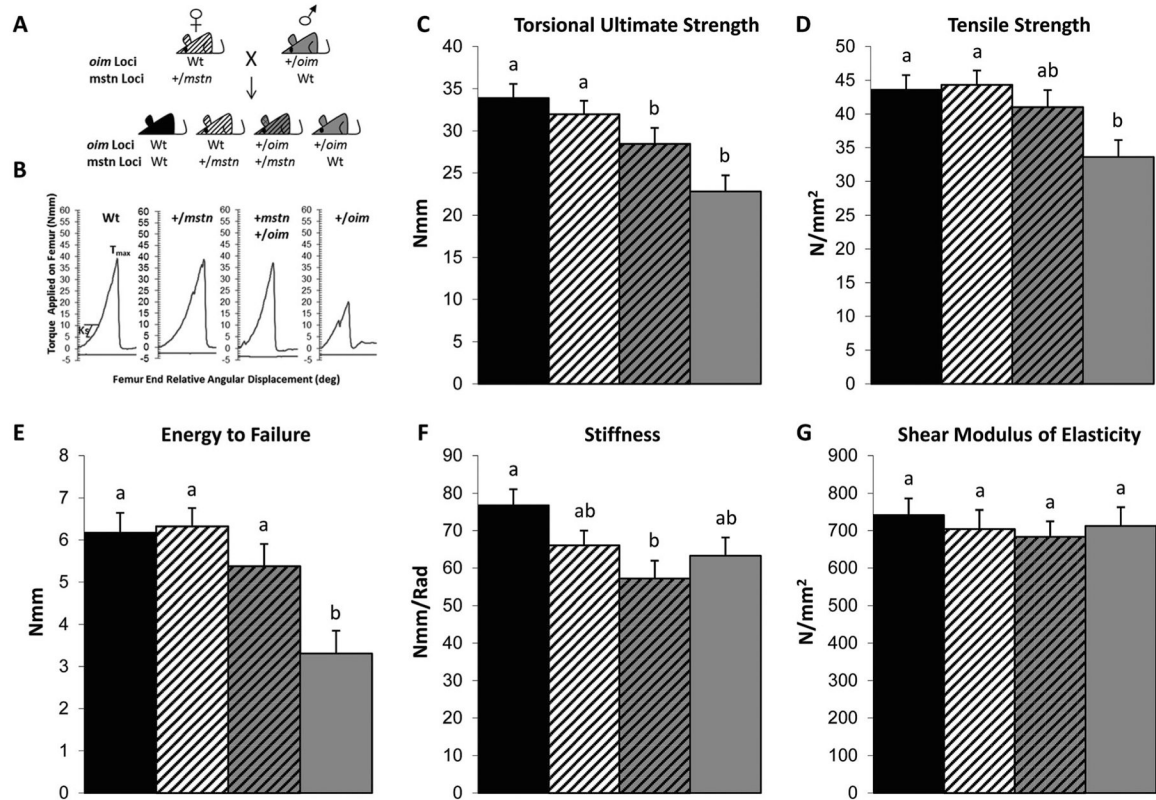
Fig. 1.
A Schematic of the +/*mstn* (dam) X +/*oim* (sire) mice breeding scheme with the resultant genotypes of the offspring indicated. **B** Representative graphs showing the torque applied on the femur of Wt, +/*mstn*, +/*mstn* +/*oim*, and +/*oim* offspring per angular displacement. **B–G** Myostatin deficiency partially rescues the bone phenotype of +/*oim* mice as seen in 4-month-old +/*mstn* +/*oim* femora. **C** Torsional ultimate strength (T_{max}), **D** tensile strength (Su), **E** energy to failure (U), **F** torsional stiffness (Ks), **G** shear modulus of elastcity. The genotype main effect was evaluated. Values are the LSmeans±SE of the combined genotype values regardless of sex. Values with the same *superscript letter* are not significantly different. Differences were considered significant at *p* 0.05. Wt (*solid black*), *n*=21; +/*mstn* (*black and white*), *n*=25–26; +/*mstn*, +/*oim* (*black and gray*), *n*=18; +/*oim* (*gray*), *n*=18
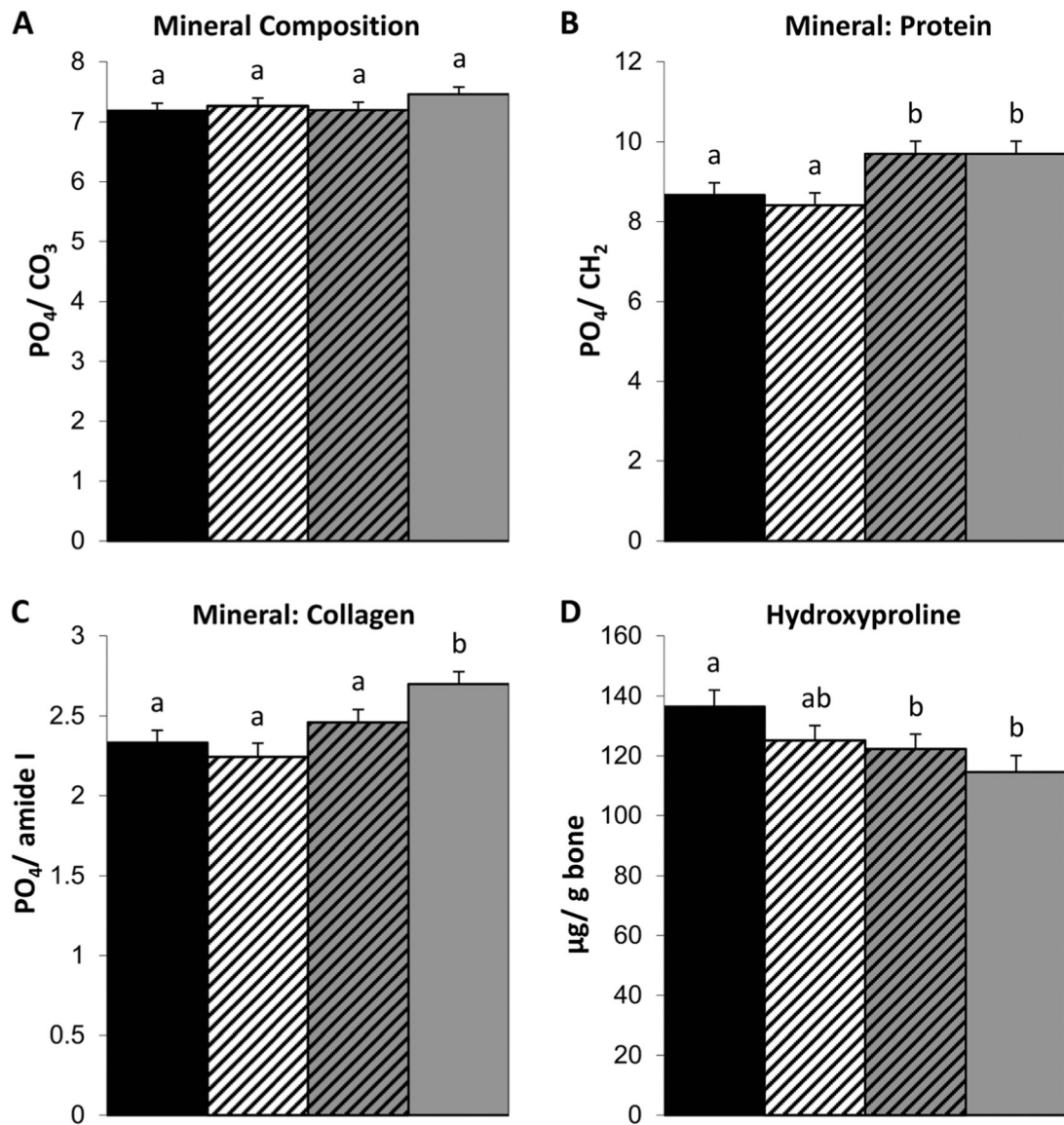
Fig. 2.
Myostatin deficiency in 4-month-old +/*mstn* +/*oim* tibiae increases the PO_4/amide I (mineral to collagen) ratio as compared to +/*oim* tibiae. Cortical bone **A** PO_4/CO_3 ratio (indication of carbonate substitution of phosphate in the crystal lattice), **B** PO_4/CH_2 ratio (relative amount of mineral phosphate to matrix protein), **C** PO_4/amide I ratio (relative amount of mineral to collagen), and **D** femoral hydroxyproline content (μg/g bone). The genotype main effect was evaluated. Values are the LSmeans±SE of the combined genotype values regardless of sex. Values with the *same superscript letter* are not significantly different. Differences were considered significant at *p* 0.05. Wt (*solid black*), *n*=13–14; +/*mstn* (*black and white*), *n*=11–17; +/*mstn*, +/*oim* (*black and gray*), *n*=12–17; +/*oim* (*gray*), *n*=13–14
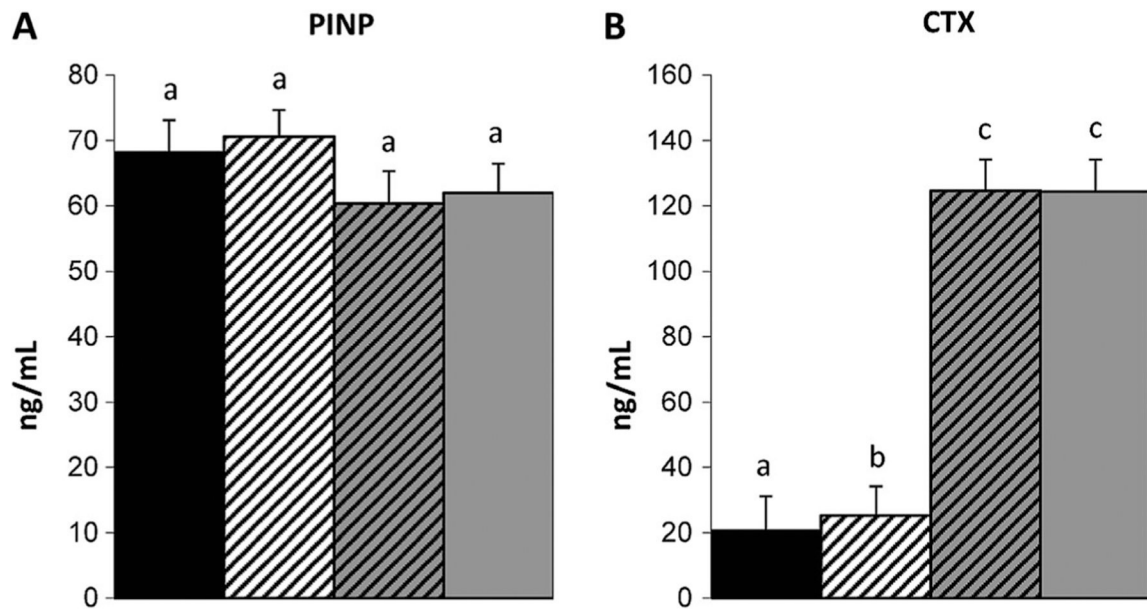
Fig. 3.
Evaluation of serum bone turnover markers, N-terminal propeptide of type I procollagen [PINP (**A**)] and C-terminal cross-linked telopeptide of type I collagen [CTX (**B**)] demonstrated an increase in serum CTX associated with +/*oim* and +/*mstn* +/*oim* mice. The genotype main effect was evaluated. Values are the LSmeans±SE of the combined genotype values regardless of sex. Values with the same *superscript letter* are not significantly different. Differences were considered significant at *p* 0.05. Wt (*solid black*), *n*=13; +/*mstn* (*black and white*), *n*=16–19; +/*mstn*, +/*oim* (*black and gray*), *n*=17–18; +/*oim* (*gray*), *n*=15–16

Table 1

Body and hindlimb muscle and relative muscle weights of adult 4-month-old offspring of +/*mstn* X +/*oim* crosses

Parameter	Wt n=24–27	+/mstn n=32–34	+/mstn +/oim n=35	+/oim n=27
Body weight (g)	27.26±0.46[a]	28.55±0.42[b]	28.74±0.41[b]	25.91±0.46[c]
Muscle wet weight (mg)				
Soleus	8.51±0.36[a]	10.20±0.32[b]	9.64±0.30[b]	8.24±0.34[a]
Plantaris	18.01±0.54[a]	21.31±0.48[b]	21.15±0.45[b]	16.72±0.51[a]
Gastrocnemius	123.4±3.6[a]	147.9±3.2[b]	140.1±3.0[b]	120.1±3.4[a]
Tibialis anterior	49.27±1.73[a]	58.89±1.54[b]	59.67±1.43[b]	49.97±1.63[a]
Quadriceps	197.4±6.0[a]	232.0±5.3[b]	232.0±5.0[b]	198.5±5.6[a]
Relative wet muscle weight [wet weight (mg)/body weight (g)]				
Soleus	0.032±0.001[a]	0.036±0.001[b]	0.034±0.001[ab]	0.032±0.001[a]
Plantaris	0.068±0.002[a]	0.074±0.002[b]	0.074±0.002[b]	0.064±0.001[a]
Gastrocnemius	0.467±0.013[a]	0.516±0.012[b]	0.487±0.011[ab]	0.465±0.013[a]
Tibialis anterior	0.187±0.007[a]	0.207±0.006[b]	0.209±0.006[b]	0.195±0.007[ab]
Quadriceps	0.748±0.022[a]	0.808±0.020[b]	0.803±0.019[ab]	0.767±0.021[ab]

Data were evaluated by analysis of variance and no genotype and sex interactions were found.

The genotype main effect was evaluated, and the values expressed are the LSmeans±SE of the combined genotype values regardless of sex. Values within a row with the same superscript letter are not significantly different. Differences were considered significant at p 0.05

Table 2

Tibial microarchitecture of 4-month-old male offspring from +/*mstn* x +/*oim* crosses

Parameter	Wt n=15	+/mstn n=12	+/mstn +/oim n=12	+/oim n=12
Trabecular bone				
BV/TV	0.166±0.009[a]	0.224±0.010[b]	0.182±0.010[a]	0.154±0.010[a]
Number (1/mm)	4.41±0.14[a]	4.94±0.15[b]	4.30±0.15[ac]	3.96±0.15[c]
Density (mg HA/CCM)	833.6±7.1[a]	790.7±7.9[b]	804.3±7.8[b]	857.8±7.8[c]
Connectivity density	97.4±7.6[a]	131.1±8.5[b]	99.2±8.4[a]	74.6±8.4[c]
SMI	1.84±0.08[a]	1.52±0.09[b]	1.91±0.09[a]	2.04±0.09[a]
Thickness (mm) *				
Male (n=6–8)	0.055±0.002[a]	0.064±0.001[b]	0.063±0.002[b]	0.057±0.003[a]
Female (n=6–7)	0.052±0.001[a]	0.052±0.001[a]	0.055±0.002[a]	0.056±0.002[a]
Separation (1/mm) *				
Male (n=6–8)	0.164±0.003[a]	0.150±0.011[a]	0.166±0.006[a]	0.175±0.007[a]
Female (n=6–7)	0.307±0.012[a]	0.285±0.023[a]	0.366±0.032[b]	0.394±0.017[b]
Cortical bone				
Thickness (mm)	0.227±0.003[a]	0.224±0.004[ab]	0.216±0.004[b]	0.216±0.003[b]
Density (mg HA/CCM)	1129.5±8.8[a]	1088.8±9.7[b]	1115.0±9.6[ab]	1149.3±9.3[a]

Data were evaluated by analysis of covariance with body weight as the covariate

*
When genotype and sex interactions were significant, male and female values are expressed as means±SE. If the genotype and sex interaction were not significant, the genotype main effect was evaluated, and the values expressed are the LSmeans±SE of the combined genotype values regardless of sex. Values within a row with the same superscript letter are not significantly different. Differences were considered significant at p 0.05

Table 3

Femoral geometry of adult 4-month-old offspring of +/*mstn* X +/*oim* crosses

Geometric parameter	Wt *n=21*	+/*mstn n=26*	+/*mstn* +/*oim n=20*	+/*oim n=18*
Femur length (mm)	16.18±0.08[a]	15.96±0.08[a]	16.11±0.09[a]	16.05±0.09[a]
Marrow cavity diameter (mm)	0.91±0.02[a]	0.87±0.02[a]	0.81±0.02[b]	0.77±0.03[b]
Cortical bone width (mm)	0.41±0.01[a]	0.41±0.01[a]	0.43±0.01[a]	0.44±0.01[a]
Polar moment of inertia (mm⁴)	0.76±0.03[a]	0.69±0.03[ac]	0.63±0.04[b]	0.65±0.04[bc]

Data were evaluated by analysis of covariance with body weight as the covariate. No genotype and sex interactions were found.

The genotype main effect was evaluated, and the values expressed are the LSmeans±SE of the combined genotype values regardless of sex. Values within a row with the same superscript letter are not significantly different. Differences were considered significant at *p* 0.05